


 Cite this: *RSC Adv.*, 2026, 16, 1612

# A high-energy-density and low-waste battery for energy source transition from C-, H-, and O-based material era to H- and O-based material era

 Yingpeng Zhen<sup>†\*a</sup> and Yansong Zhao<sup>ID †\*b</sup>

The discovery of an ideal energy source is always a dream for humans since ancient times. Wood, coal, petroleum and natural gas have played an important role as energy sources in the long history of humans, even at present. However, they are C-, H-, and O-based energy sources, which cause the emission of greenhouse gas CO<sub>2</sub>. Therefore, the whole world is always searching for a low-emission or zero-emission energy source. Currently, hydrogen and battery technologies are the two key energy solutions for CO<sub>2</sub> emission reduction. Hydrogen technology can use water as a raw material to produce H<sub>2</sub>, which seems to be an ideal solution for low- or zero-emission. However, hydrogen technology has the drawback of low energy conversion efficiency, as well as hydrogen storage and transportation issues. Current battery technology including Li-ion batteries and Na-ion batteries suffers from the disadvantages of battery waste, low safety, low charge speed, and high costs. In this work, in order to overcome the disadvantages of hydrogen and battery technologies, we developed a high-energy-density super flow battery powered by hydrogen peroxide, a kind of zero-emission and low-waste H- and O-based energy source, for energy storage and supply. Unlike conventional one-stage redox flow batteries, the super flow battery has two stages to improve its energy density. We utilized hydrogen peroxide as a catholyte regeneration agent in the second-stage tank of the super flow battery to significantly increase its energy density. We found that the energy density of hydrogen peroxide catholyte regeneration agents and Na<sub>2</sub>S anolyte materials reached 305 Wh kg<sup>-1</sup> and 421 Wh kg<sup>-1</sup>, respectively, using the two-stage structure of the super flow battery, which endowed the super flow battery with a higher energy density than that of the Li-ion and conventional flow batteries.

 Received 16th November 2025  
 Accepted 22nd December 2025

DOI: 10.1039/d5ra08850j

[rsc.li/rsc-advances](http://rsc.li/rsc-advances)

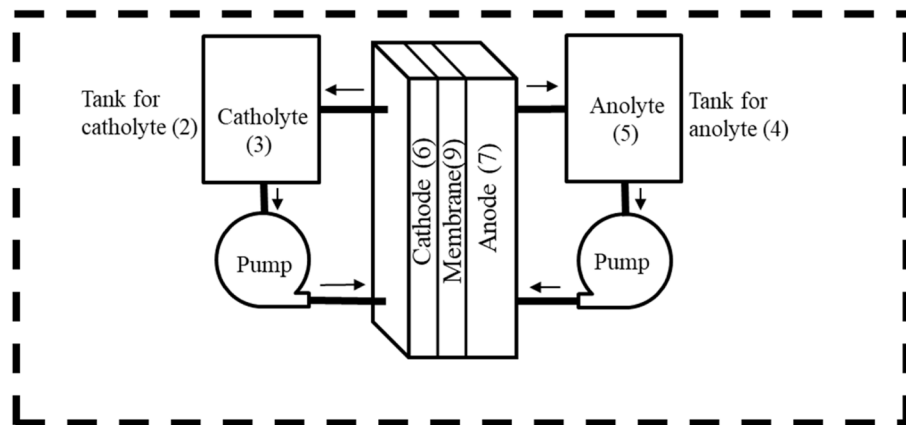
## Introduction

Finding an ideal energy source is always a dream for humans since ancient times.<sup>1–15</sup> Currently, the climate change issue raises increasing concerns. In order to replace fossil fuels, a C-, H-, and O-based energy source, hydrogen technology<sup>8,16–18</sup> and battery technology<sup>19–22</sup> are paid much attention, which have become the two key energy solutions for CO<sub>2</sub> emission reduction. In the history of humans, many researchers have made attempts to use low-cost and abundant water as the raw material for energy. Green hydrogen is a clean energy solution that produces hydrogen using water and renewable energy sources. However, the energy conversion efficiency of green hydrogen is low. In addition, hydrogen has serious storage and transportation issues.<sup>17</sup> Therefore, Li-ion batteries have gained great

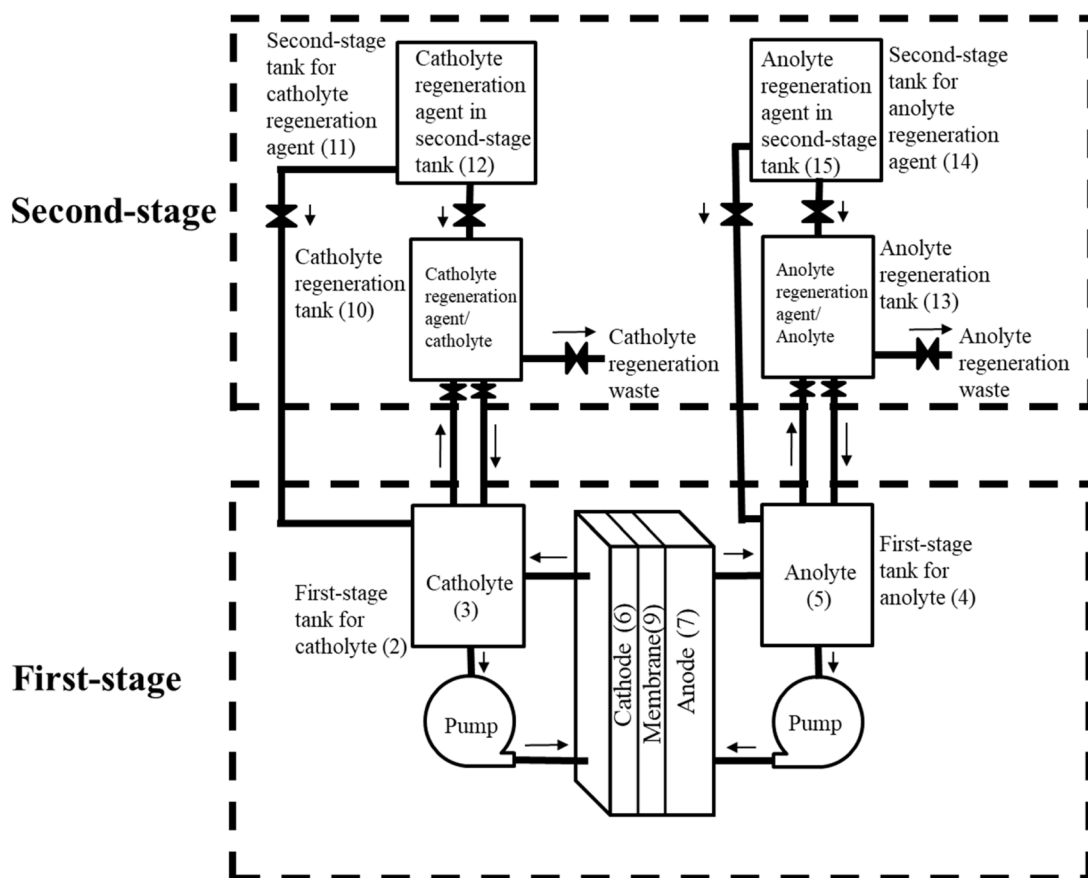
attention for storing energy obtained from renewable energy sources.<sup>19,20</sup> Li-ion batteries have been increasingly used for energy storage applications due to their ability to store and release electricity. However, Li-ion-based batteries still have many disadvantages, for example, high costs of the raw materials, safety issues, limited Li resources on earth, and battery waste issue. The safety issues of Li-ion-based batteries are mainly related to fire and explosion risks since the battery is highly active and sensitive to water and oxygen. The organic solvents in Li-ion batteries are flammable, and there have been several incidents of Li-ion-based battery explosion reported in the past. The Li-ion battery causes no emission upon its use, but there are a lot of CO<sub>2</sub> emissions during its production. After the Li-ion battery is dead, battery waste treatment is costly, and it results in a serious CO<sub>2</sub> emission issue and environmental problem. Therefore, many researchers try to develop new types of batteries to replace Li-ion batteries. However, the above-mentioned disadvantages of Li-ion batteries still remain in other types of batteries.

Many researchers are also trying to use redox-flow batteries for energy storage. As shown in Fig. 1a, the conventional flow battery is an electrochemical energy storage system that stores

<sup>a</sup>Atomcent Holding AS, 5184 Bergen, Norway. E-mail: [yingpeng.zhen@atomcent.com](mailto:yingpeng.zhen@atomcent.com); [ypzhen521@gamil.com](mailto:ypzhen521@gamil.com)
<sup>b</sup>Department of Safety, Chemistry and Biomedical Laboratory Sciences, Western Norway University of Applied Sciences (HVL), 5063 Bergen, Norway. E-mail: [yansong.zhao@hvl.no](mailto:yansong.zhao@hvl.no); [yansong.zhao2004@gmail.com](mailto:yansong.zhao2004@gmail.com)
<sup>†</sup> Dr Zhen and Dr Zhao are co-first authors and co-corresponding authors.

(a)



(b)

Fig. 1 Structure of (a) conventional flow battery and (b) super flow battery.

electrical energy in the chemical form by using two liquid electrolytes stored in separate tanks. The catholyte and anolyte are pumped through a reaction cell, where they undergo

electrochemical reactions, generating electricity. The conventional flow battery has the following advantages for energy storage: (1) long cycle life (>30 years or >20 000 charge/discharge



cycles); (2) open system: flow battery is an open system for energy conversion during charge and discharge processes. A lot of physical and chemical operations can be utilized to improve the flow battery performance during charge and discharge processes in the whole flow battery lifespan. (3) Scalability: the energy capacity of the flow battery can be easily adjusted by increasing or decreasing the size of the electrolyte tanks and adjusting the flow rates of the electrolytes. (4) High efficiency: flow batteries can achieve a high round-trip efficiency, which is the ratio of energy output to input during charge and discharge cycles. This efficiency can be competitive with other energy storage technologies. (5) Safe operation: flow batteries are very safe, as the separation of the electrolytes by a membrane reduces the risk of thermal runaway or fire, which can be a concern with some other battery types. (6) Environment-friendliness: flow battery chemistry uses non-toxic and environmentally friendly electrolyte materials, which can be an advantage from an environmental and safety perspective. (7) Simple structure and easy maintenance. (8) Electrical grid integration: flow batteries are well suited for electrical grid integration, renewable energy smoothing, and energy shifting, helping to stabilize and optimize the performance of electrical grids with intermittent renewable energy sources like wind and solar.

However, the main disadvantage of conventional flow batteries in energy storage is the low energy density.<sup>13</sup> One of the main reasons for the low energy density of conventional flow batteries is as follows: conventional flow battery is a type of one-stage flow battery, which utilizes electric chargeable catholytes and anolytes in one-stage tanks to store energy (as shown in Fig. 1a). However, there is a solubility limitation of chargeable materials in the catholyte or anolyte solution (normally around 1–2 mol L<sup>-1</sup>) of conventional flow batteries, which endows the conventional flow battery with low energy density, normally less than 70 Wh L<sup>-1</sup>. This limits the application of flow batteries in energy storage devices for mobility, for example, electric vehicles (EVs). Due to the one-stage structure, the conventional flow battery shows a disadvantage of low energy density. Therefore, the conventional flow battery is currently utilized in stationary large-scale energy storage and not mobile energy storage. However, normally, high-cost metal elements should be utilized to prepare electrolytes for the conventional flow battery; hence, large-scale energy storage is expensive.

In this work, we designed and utilized a new type of super flow battery for energy storage to reduce CO<sub>2</sub> emissions, overcoming the disadvantages of hydrogen technology, Li-ion batteries and conventional flow batteries. We significantly improved the energy density of the super flow battery. Unlike the conventional flow battery, this super flow battery has two stages. The structure of two-stage super flow battery is shown in Fig. 1b. The two-stage structure of the super flow battery can significantly increase its energy density. For example, our hydrogen peroxide-powered super flow battery can reach a catholyte energy density of 305 Wh kg<sup>-1</sup> and an anolyte energy density of 421 Wh kg<sup>-1</sup>, which are higher than the energy density of the Li-ion battery available on the market. Actually, the theoretical energy density of H<sub>2</sub>O<sub>2</sub> is 1577 Wh kg<sup>-1</sup>. Besides

the eight above-mentioned advantages of the conventional flow battery, our hydrogen peroxide-powered super flow battery has advantageous properties as follows: (1) low-waste: there is almost no battery waste in this super flow battery. The only main wastes released are H<sub>2</sub>O and O<sub>2</sub> during the super flow battery working process. (2) Extremely high energy density (catholyte energy density of 305 Wh kg<sup>-1</sup> and anolyte energy density of 421 Wh kg<sup>-1</sup>). (3) Discharged catholyte can be regenerated/charged quickly (less than 1 minute) by hydrogen peroxide. (4) Profitable battery discharge process. In the anolyte side, the discharged anolyte (Na<sub>2</sub>S<sub>x</sub> solution) can be replaced by a fresh Na<sub>2</sub>S anolyte quickly (less than 1 minute). Product of anolyte discharged Na<sub>2</sub>S<sub>x</sub> is more expensive than Na<sub>2</sub>S in anolyte side, which leads to super flow battery can make money during electricity producing for energy supply. The product Na<sub>2</sub>S<sub>x</sub> can be utilized in many fields, including rubber industry, textile industry, mining and metallurgy,<sup>23</sup> chemical synthesis and reagents, sodium-sulfur batteries,<sup>24</sup> and lithium-sulfur batteries.<sup>25</sup> (5) H and O-based energy carriers are much cheaper than metal element-based energy carriers for flow batteries in energy storage. Hydrogen peroxide can be utilized for energy storage to power the super flow battery for energy supply to stationary and mobile devices. H and O of hydrogen peroxide is derived from H<sub>2</sub>O, which helps realize the use of H<sub>2</sub>O as the raw material for energy storage. Therefore, our super flow battery technology has high potential to replace Li-ion batteries, hydrogen technology and other energy storage technologies for mobile and stationary energy storage applications.

## Experimental

### Preparation of the two-stage super flow battery

A two-stage super flow battery is shown in Fig. 1b. A typical two-stage super flow battery includes two stages according to the total stage numbers of tanks. First stage of super flow battery (as shown in Fig. 1b) consists of: first-stage tank for catholyte, catholyte, first-stage tank for anolyte, anolyte, cathode, anode, porous materials, ion exchange membrane, frame, and gasket. Second-stage of super flow battery (as shown in Fig. 1b) consists of: catholyte regeneration tank, second-stage tank for catholyte regeneration agent, catholyte regeneration agent in second-stage tank, anolyte regeneration tank, second-stage tank for anolyte regeneration agent, and anolyte regeneration agent in second-stage tank. The cathode and anode of the super flow battery in this example is graphite. The ion-exchange membrane is a Nafion film. The catholyte is a V<sup>5+</sup>/V<sup>4+</sup> solution, and the anolyte is a Na<sub>2</sub>S solution. The catholyte regeneration agent is H<sub>2</sub>O<sub>2</sub>.

### Preparation of the catholyte

The catholyte is prepared as follows: (1) a H<sub>2</sub>SO<sub>4</sub> aqueous solution was prepared. The concentration of H<sub>2</sub>SO<sub>4</sub> aqueous solution was 3 mol L<sup>-1</sup>. (2) VOSO<sub>4</sub> was dissolved into the H<sub>2</sub>SO<sub>4</sub> aqueous solution to obtain a 3 mol per L VOSO<sub>4</sub> solution as the catholyte. The catholyte regeneration agent in the second-stage tank was H<sub>2</sub>O<sub>2</sub> with 30 wt% in water.



## Preparation of the anolyte

Na<sub>2</sub>S with a mass fraction purity ranging from 60% to 64% was utilized to prepare the anolyte solution. The anolyte was 2 mol per L Na<sub>2</sub>S aqueous solution. Then, 1 mol per L NaOH was added into the anolyte to avoid H<sub>2</sub>S release from the anolyte solution during the discharge process.

## Catholyte regeneration

Before the super flow battery started working, 33 mL of 3 mol per L VOSO<sub>4</sub> catholyte was added into the catholyte tank. Subsequently, 5.67 g H<sub>2</sub>O<sub>2</sub> was added into the catholyte tank and mixed with the VOSO<sub>4</sub> catholyte to oxidize V<sup>4+</sup> (VO<sup>2+</sup>) to V<sup>5+</sup>. VO<sup>2+</sup> was in the low-energy status and V<sup>5+</sup> was in the high-energy status. Thus, the catholyte was converted to high-energy status by H<sub>2</sub>O<sub>2</sub>. H<sub>2</sub>O<sub>2</sub> is a clean oxidant. The only possible wastes from H<sub>2</sub>O<sub>2</sub> as the catholyte regeneration agent are H<sub>2</sub>O and O<sub>2</sub>. During the discharge process, the catholyte V<sup>5+</sup> was converted into V<sup>4+</sup> and the anolyte Na<sub>2</sub>S was converted into Na<sub>2</sub>S<sub>x</sub>. Meanwhile, the catholyte regeneration agent H<sub>2</sub>O<sub>2</sub> from the second-stage tank was added/pumped into the catholyte regeneration tank or the first-stage tank for the catholyte with V<sup>5+</sup> and V<sup>4+</sup> to convert V<sup>4+</sup> into V<sup>5+</sup> in order to keep high-energy status V<sup>5+</sup> at a high concentration level in the catholyte. At the same time, H<sub>2</sub>O<sub>2</sub> was converted into H<sub>2</sub>O or O<sub>2</sub>. After a certain period of super flow battery discharge process, due to the converted water from H<sub>2</sub>O<sub>2</sub> in the catholyte regeneration process, the whole or part of the catholyte was pumped into the catholyte regeneration tank to remove the excess water by reverse osmosis. At the same time, the pH of the catholyte was tested and regulated by the pH regulation agent.

## Discharged anolyte (NaS<sub>x</sub>) collection

The saturated NaS<sub>x</sub> was collected and pumped out from the anolyte tank. Subsequently, the fresh Na<sub>2</sub>S anolyte was pumped into the anolyte tank.

## Battery discharge test

The discharge performance of the super flow battery was tested using a Battery Testing System. The programme utilized during the discharge is as follows: (a) rest period (at least 30 seconds): the system has a rest for at least 30 seconds prior to the first discharge cycle. This process is to make sure the super flow battery is in a stable status after catholyte regeneration with H<sub>2</sub>O<sub>2</sub>. (b) Discharge at a constant current (10 mA): the discharge phase begins at a constant current of 10 mA, until the voltage reaches 0.4 V. This controlled discharge at low discharge currents allows for the steady release of stored energy from the battery. (c) Discharge at a constant current (5 mA): the discharge phase begins at a constant current of 5 mA, until the voltage reaches 0.4 V. This controlled discharge at low discharge currents allows for a steady release of stored energy from the battery. (d) Discharge at a constant current (1 mA): the discharge phase begins at a constant current of 1 mA.

## Energy density calculation

The energy density of the catholyte regeneration agent (H<sub>2</sub>O<sub>2</sub>) was calculated as follows. The mass of H<sub>2</sub>O<sub>2</sub> is *m*. The mass fraction concentration of H<sub>2</sub>O<sub>2</sub> is *a*%. The discharge capacity (*C<sub>d</sub>*) and average voltage (*V*) of the battery can be obtained using the battery testing system. The energy density (*E<sub>m</sub>*) of H<sub>2</sub>O<sub>2</sub> is *E<sub>m</sub>* = *C<sub>d</sub>* × *V*/(*m* × *a*%). The energy density of Na<sub>2</sub>S can also be calculated using the similar method.

## UV-vis test

The UV-vis curves of the samples were tested at a wavelength ranging from 400 nm to 1100 nm at room temperature.

## FTIR test

The FTIR test of the samples was performed with a wavenumber ranging from 500 cm<sup>-1</sup> to 4000 cm<sup>-1</sup> at room temperature.

## Results and discussion

In this work, 3 M VOSO<sub>4</sub> in 3 M H<sub>2</sub>SO<sub>4</sub> aqueous solution was utilized as the catholyte and 2 M Na<sub>2</sub>S aqueous solution was utilized as the anolyte in the first-stage tanks of the super flow battery. Then, 30 wt% hydrogen peroxide in water was utilized as the catholyte regeneration agent in the second-stage tank of the super flow battery. First, VOSO<sub>4</sub> (as shown in Fig. 2a) and 3 M H<sub>2</sub>SO<sub>4</sub> were mixed together to form a 3 M VOSO<sub>4</sub> catholyte (as shown in Fig. 2b). VO<sup>2+</sup> is one of the most stable double-atom ion. Before the super flow battery started working, 33 mL of 3 M VOSO<sub>4</sub> catholyte was added into the catholyte regeneration tank. Subsequently, 5.67 g hydrogen peroxide (30 wt%) in water in the catholyte regeneration agent tank was added into the catholyte tank and mixed with the VOSO<sub>4</sub> catholyte to oxidize VO<sup>2+</sup> (V<sup>4+</sup>) to V<sup>5+</sup>. Hydrogen peroxide underwent a rapid and significant reaction with V<sup>4+</sup> to form V<sup>5+</sup>. Only one drop of hydrogen peroxide (30 wt%) in water leads to colour change of 3 M VOSO<sub>4</sub> significantly from blue to dark blue (as shown in Fig. 2c). V<sup>4+</sup> was in the low-energy status and V<sup>5+</sup> was in the high-energy status. After V<sup>4+</sup> was oxidized into V<sup>5+</sup> by 5.67 g 30 wt% hydrogen peroxide, the bulk ion was V<sup>5+</sup> in the catholyte solution and the colour of the catholyte solution became dark black (as shown in Fig. 2d). By this way, the catholyte is converted into high-energy status by H<sub>2</sub>O<sub>2</sub> from the low-energy status. H<sub>2</sub>O<sub>2</sub> is a clean oxidant. The only possible emissions or wastes from H<sub>2</sub>O<sub>2</sub> as the catholyte regeneration agent are H<sub>2</sub>O and O<sub>2</sub>. When H<sub>2</sub>O<sub>2</sub> was utilized, the possible decomposition of H<sub>2</sub>O<sub>2</sub> by light or metal ion should be paid attention to. For example, a light-proof plastic container should be used to store H<sub>2</sub>O<sub>2</sub>. In addition, metal-ion pollutants should be avoided in H<sub>2</sub>O<sub>2</sub>. Moreover, a H<sub>2</sub>O<sub>2</sub> stabilizer should be utilized when necessary. During the discharge process, the catholyte V<sup>5+</sup> was converted into V<sup>4+</sup> with blue colour (as shown in Fig. 2e). The catholyte regeneration agent H<sub>2</sub>O<sub>2</sub> from the second-stage tank was added into the first-stage tank for the catholyte with V<sup>5+</sup> and V<sup>4+</sup> to convert V<sup>4+</sup> into V<sup>5+</sup> in order to keep the high-energy status V<sup>5+</sup> at a high concentration level in catholyte. At the same time, H<sub>2</sub>O<sub>2</sub> was converted into H<sub>2</sub>O or O<sub>2</sub>.



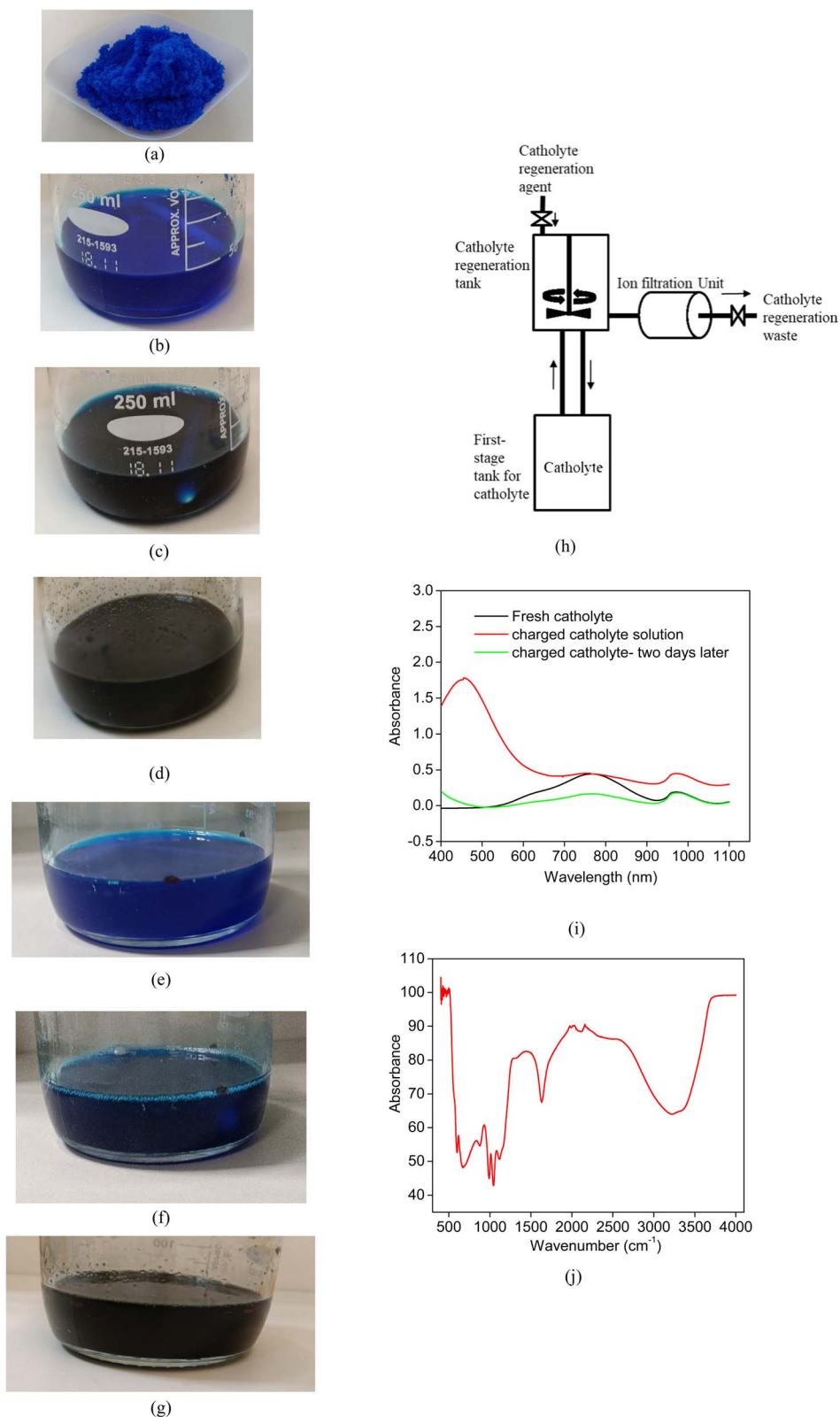


**Fig. 2** Catholyte regeneration: (a) VOSO<sub>4</sub>; (b) 3 M VOSO<sub>4</sub> in a 3 M H<sub>2</sub>SO<sub>4</sub> aqueous solution; (c) one drop hydrogen peroxide in the sample of 3 M VOSO<sub>4</sub> in a 3 M H<sub>2</sub>SO<sub>4</sub> aqueous solution; (d) 3 M VOSO<sub>4</sub> in a 3 M H<sub>2</sub>SO<sub>4</sub> aqueous solution is fully oxidized; (e) 3 M VOSO<sub>4</sub> in 3 M H<sub>2</sub>SO<sub>4</sub> aqueous solution is fully oxidized and fully discharged; (f) one drop hydrogen peroxide in the fully discharged sample of 3 M VOSO<sub>4</sub> in 3 M H<sub>2</sub>SO<sub>4</sub> aqueous solution; (g) regenerated VOSO<sub>4</sub> after 10 cycles of regeneration by hydrogen peroxide; (h) cathode regeneration process; (i) UV-vis spectra of the VOSO<sub>4</sub> solution, fully charged VOSO<sub>4</sub> solution, and fully charged samples two days later; and (j) FTIR spectra of the VOSO<sub>4</sub> solution.



After one drop of  $\text{H}_2\text{O}_2$  was added into the fully discharged sample in blue colour, as shown in Fig. 2f, the colour of the sample changed significantly to dark black, as shown in Fig. 2e. However, after 2 g  $\text{H}_2\text{O}_2$  was added into the fully discharged sample, as shown in Fig. 2e, the sample turned dark black, as shown in Fig. 2g, the colour of which is the same as the colour of the sample shown in Fig. 2e. This means that the fully discharged catholyte was fully charged now. Using  $\text{H}_2\text{O}_2$ ,  $\text{V}^{4+}$  and  $\text{V}^{5+}$  can be reversibly converted during the charge and discharge process of this super flow battery. The only consumed energy source in the catholyte charge process of this super flow battery is  $\text{H}_2\text{O}_2$ , not electricity. After a certain period of super flow battery discharge process, whole or part of the catholyte was pumped into the catholyte regeneration tank to remove the excess water due to the converted water from  $\text{H}_2\text{O}_2$  in the catholyte regeneration process *via* the reverse osmosis technology (as shown in Fig. 2h). At the same time, the pH of catholyte was tested and regulated by pH regulation agent. The UV-vis spectra of  $\text{VOSO}_4$  (fresh catholyte),  $\text{VOSO}_4$  + hydrogen peroxide (charged catholyte solution), and charge catholyte after two days are shown in Fig. 2i. The charged catholyte solution had an absorption peak at 456 nm, which confirmed the formation of  $\text{V}^{5+}$  ion<sup>26</sup> with the mixed  $\text{H}_2\text{O}_2$  and  $\text{VOSO}_4$  sample.  $\text{H}_2\text{O}_2$  oxidized  $\text{V}^{4+}$  ( $\text{VO}^{2+}$ ) into  $\text{V}^{5+}$ . The charged catholyte solution was kept quiescently on the laboratory table for two days. Subsequently, UV-vis spectroscopy was performed. As shown in Fig. 2i, there was no peak at 456 nm for the UV-vis curve of the charged catholyte solution after two days, like fresh catholyte, which indicated that  $\text{V}^{5+}$  was spontaneously converted into  $\text{V}^{4+}$ . This result also manifests that  $\text{V}^{5+}$  can spontaneously become  $\text{V}^{4+}$  during the discharge process of the super flow battery. The FTIR curves of the  $\text{VOSO}_4$  solution are shown in Fig. 2j. There was a strong absorption peak at  $990\text{ cm}^{-1}$ , which was assigned to the  $\text{V}(+4)=\text{O}$  stretching vibration and proved the presence of  $\text{VO}^{2+}$  in the  $\text{VOSO}_4$  solution. In addition, in the FTIR curve, we can find a strong absorption peak at  $1100\text{ cm}^{-1}$  due to the presence of  $\text{SO}_4^{2-}$  in the  $\text{VOSO}_4$  solution.

Unlike the conventional one-stage redox flow battery, the catholyte in the first stage of super flow battery was not electrically charged directly, which was regenerated (charged) by the hydrogen peroxide catholyte regeneration agent from the second-stage tank of the super flow battery during the entire discharge process. The catholyte in the first stage of the super-flow battery worked as a “medium” to generate electric energy from the catholyte regeneration agent in the second-stage tank of the super flow battery during the discharge process. The catholyte can be regenerated (charged) by the catholyte regeneration agent from low-energy status to high-energy status (from  $\text{V}^{4+}$  to  $\text{V}^{5+}$ ) during the discharge process (as shown in Fig. 1b). The solubility and concentration of the chargeable/dischargeable material vanadium ion in the catholyte will not influence the energy density of the super flow battery. The vanadium ion in the catholyte can be recycled to use. Compared with conventional metal element based flow battery, super flow battery only use expensive metal based catholyte as a “medium” for redox reaction of vanadium ion and therefore does not need

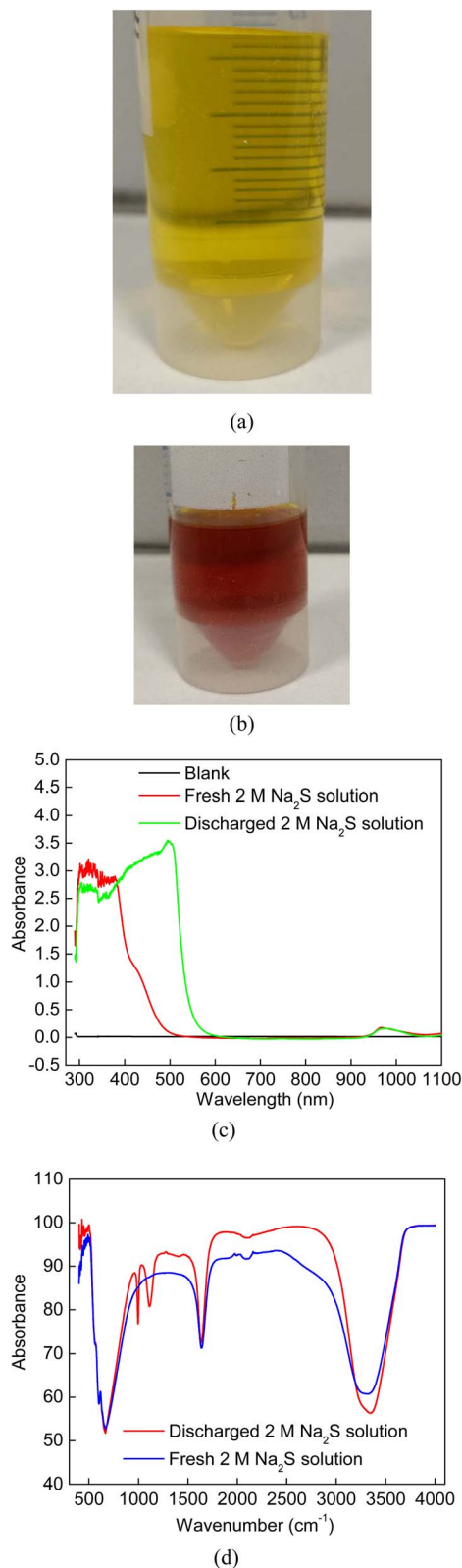


Fig. 3 Anolyte regeneration: (a) original 2 M  $\text{Na}_2\text{S}$  solution; (b) fully discharged 2 M  $\text{Na}_2\text{S}$  solution; (c) UV-vis spectra of the original 2 M  $\text{Na}_2\text{S}$  solution and fully discharged 2 M  $\text{Na}_2\text{S}$  solution; and (d) FTIR spectra of the original 2 M  $\text{Na}_2\text{S}$  solution and fully discharged 2 M  $\text{Na}_2\text{S}$  solution.

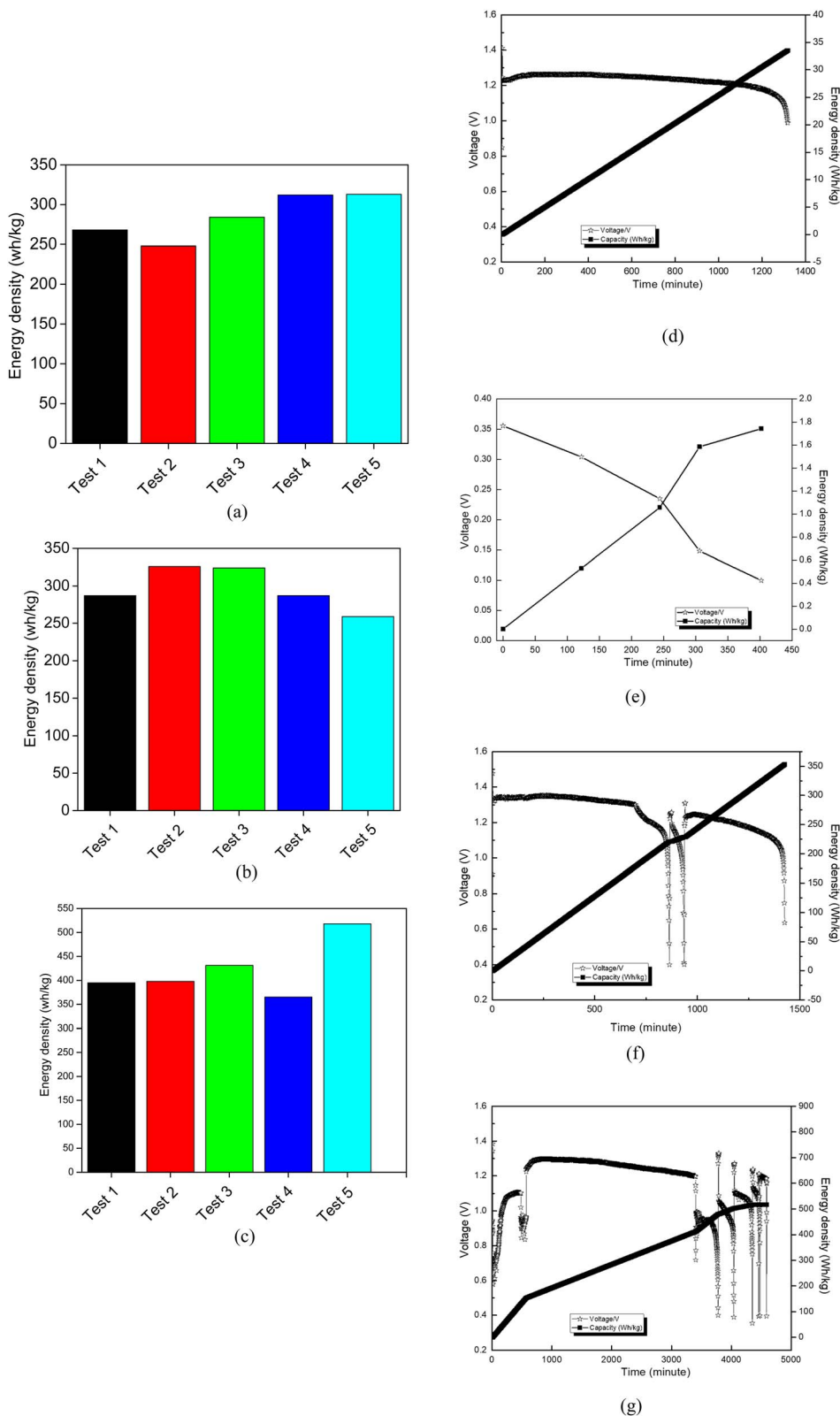


Fig. 4 Energy density test: (a) energy density test of the catholyte regeneration agent hydrogen peroxide for 5 times; (b) repeated energy density test of the catholyte regeneration agent hydrogen peroxide for 5 times; (c) energy density test of the anolyte material Na<sub>2</sub>S for 5 times; (d) energy density of the VOSO<sub>4</sub> catholyte in the conventional flow battery; (e) energy density test of hydrogen peroxide in the conventional flow battery; (f) energy density test of hydrogen peroxide in the super flow battery; and (g) energy density test of the anolyte material Na<sub>2</sub>S in the super flow battery.



so much expensive vanadium ion based catholyte for energy storage.  $\text{H}_2\text{O}_2$  and  $\text{Na}_2\text{S}$  are the energy carriers for energy storage in our super flow battery, which are much cheaper than vanadium ion-based catholytes for energy storage in the conventional flow battery.

Meanwhile, during the discharge process, the anolyte  $\text{Na}_2\text{S}$  (as shown in Fig. 3a) was converted into  $\text{Na}_2\text{S}_x$  (as shown in Fig. 3b). The colour changed from yellow to brown. The UV-vis spectra of the fresh anolyte solution (2 M  $\text{Na}_2\text{S}$  solution) and discharged anolyte solution ( $\text{Na}_2\text{S}_x$  solution) are shown in Fig. 3c. The UV-vis curve shows that there is absorption from 600 nm to 300 nm for the discharge anolyte solution, which proves the formation of  $\text{S}_8^{2-}$  and  $\text{S}_7^{2-}$ .<sup>27</sup> The FTIR curves of the fresh anolyte solution (2 M  $\text{Na}_2\text{S}$  solution) and discharged anolyte solution ( $\text{Na}_2\text{S}_x$  solution) are shown in Fig. 3d. For the discharged anolyte solution, there is a peak at  $1130\text{ cm}^{-1}$ . For the fresh anolyte, there is no peak at  $1130\text{ cm}^{-1}$ . Terminal S of  $\text{NaS}_x$  stretching vibration peak is at  $1130\text{ cm}^{-1}$ . Based on the UV-vis curves in Fig. 3c and the FTIR curves in Fig. 3d, we can confirm the formation of  $\text{NaS}_x$  in the discharged anolyte solution. The  $\text{Na}_2\text{S}_x$  product can be collected after the anolyte in the first stage of flow battery is fully discharged. The fully discharged  $\text{Na}_2\text{S}$  solution, namely  $\text{Na}_2\text{S}_x$  solution, can be replaced by the new  $\text{Na}_2\text{S}$  solution. The current market price of  $\text{Na}_2\text{S}$  (flakes, min. 60%) is 390 USD per ton. However, the price of  $\text{Na}_2\text{S}_x$  (S content min. 52%) is 950 USD per ton. The price of  $\text{H}_2\text{O}_2$  is 136 USD per ton. Based on the calculation, during the discharge process, the super flow battery can make around 1.89 USD per kWh produced electricity, and meanwhile, can supply power.

With the help of the two-stage structure of the super flow battery, the energy density of the catholyte regeneration agent  $\text{H}_2\text{O}_2$  and the anolyte material  $\text{Na}_2\text{S}$  increased significantly. The energy density of the catholyte regeneration agent hydrogen peroxide was tested 5 times. The test results are shown in Fig. 4a. The average energy density of the catholyte regeneration agent hydrogen peroxide in the 5 tests is  $285\text{ Wh kg}^{-1}$ . In addition, the energy density of the catholyte regeneration agent hydrogen peroxide was repeatedly tested 5 times in a parallel sample. The test results are shown in Fig. 4b. The average energy density of the catholyte regeneration agent hydrogen peroxide in the 5 tests is  $297\text{ Wh kg}^{-1}$ . Moreover, the energy density test of the anolyte material  $\text{Na}_2\text{S}$  was repeated 5 times. As shown in Fig. 4c, the average energy density of the anolyte material  $\text{Na}_2\text{S}$  in the 5 tests is  $421\text{ Wh kg}^{-1}$  for this two-stage super flow battery.

The present work utilized the catholyte regeneration agent hydrogen peroxide in the super flow battery to significantly increase its energy density. As shown in Fig. 4d, the energy density of the  $\text{VO}_2$  catholyte material in the conventional flow battery (one-stage flow battery) is only  $35\text{ Wh kg}^{-1}$ . The energy density of hydrogen peroxide is very low,  $1.7\text{ Wh kg}^{-1}$ , in the conventional flow battery (as shown in Fig. 4e). Using the two-stage structure of the super flow battery, the energy density of the catholyte regeneration agent  $\text{H}_2\text{O}_2$  increased to  $355\text{ Wh kg}^{-1}$  in the two-stage super flow (as shown in Fig. 4f). In addition, using the two-stage structure of the super flow battery, the

energy density of the anolyte material  $\text{Na}_2\text{S}$  reached  $518\text{ Wh kg}^{-1}$  in the two-stage super flow battery (as shown in Fig. 4g). This shows that the super flow battery has high potential to replace the Li-ion battery and other energy storage technologies for mobile and stationary energy storage applications.

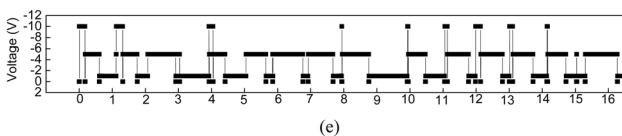
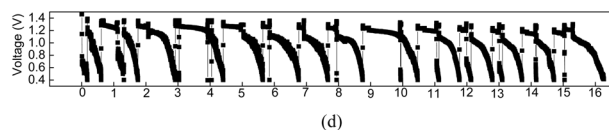
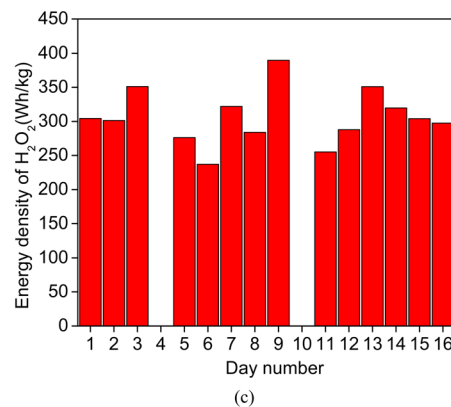
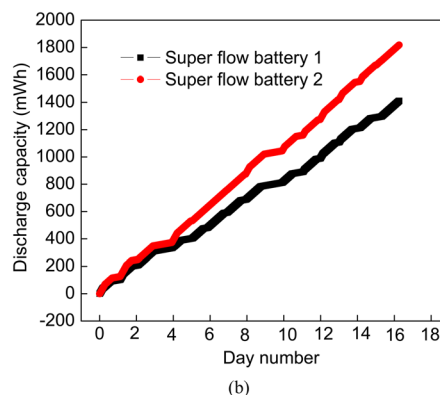
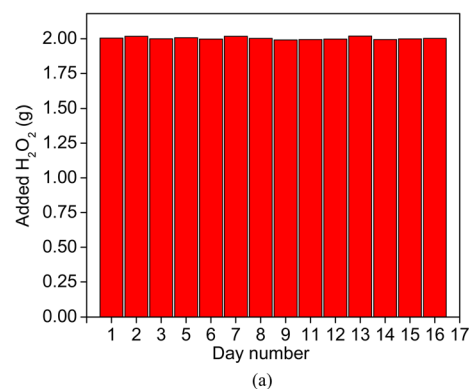


Fig. 5 Continuous discharge test of the super flow battery for 17 days: (a) added mass value of hydrogen peroxide; (b) discharge capacity of flow battery; (c) energy density of hydrogen peroxide; (d) voltage profile; and (e) current profile.



Moreover, continuous test of the super flow battery was performed for 17 days. As shown in Fig. 5a, around 2 g of 30 wt% hydrogen peroxide was added to the first-stage tank to regenerate catholyte each day from Day 1 to Day 17 (Day 4 is Sunday and Day 10 is Saturday. No 30 wt% hydrogen peroxide was added into first-stage tank in these two days). Parallel experiments of two super flow batteries were conducted. As shown in Fig. 5b, the discharge capacity of super flow battery 1 and super flow battery 2 increases continuously from Day 1 to Day 17. As shown in Fig. 5c, the average energy density of hydrogen peroxide is 305 Wh kg<sup>-1</sup> in the super flow battery. Fig. 5d shows the voltage profile of super flow battery 1 from Day 1 to Day 17. As shown in Fig. 5d, the battery can be stably discharged between 1.5 V and 0.4 V. Fig. 5e shows the current profile of super flow battery 1 from Day 1 to Day 17. As shown in Fig. 5e, the battery can be stably discharged at 10 mA, 5 mA and 1 mA.

## Conclusion

The super flow battery designed in this work solves the low energy density limitation of conventional redox flow batteries (one-stage flow battery) for energy storage. Our hydrogen peroxide-powered super flow battery shows high potential to replace the existing hydrogen technology, battery technology and conventional flow batteries for energy storage. In addition, this work opens up the possibility of using hydrogen peroxide as the energy carrier in super flow batteries to power electric devices, including electric vehicles, electrical energy bank, and charge station. Our super flow battery shortens the battery charge time to less than 1 minute. The H- and O-based energy source H<sub>2</sub>O<sub>2</sub> can be utilized as a zero-emission and low-waste fuel to charge/regenerate catholytes of super flow batteries. The discharged anolyte (Na<sub>2</sub>S<sub>x</sub> solution) can be replaced by a fresh Na<sub>2</sub>S anolyte solution to recharge/regenerate anolytes. The catholyte or anolyte recharge/regeneration can be finished within 1 minute. Moreover, this work also provides a hydrogen peroxide-powered super flow battery for large-scale energy storage in electrical grid systems. Hydrogen peroxide can be produced by H<sub>2</sub> and O<sub>2</sub> via an anthraquinone process. H<sub>2</sub> and O<sub>2</sub> can be produced from water, CH<sub>4</sub> or air. This means that water can be utilized as a raw material for energy storage. The hydrogen peroxide-powered high-energy-density super flow battery is a zero-emission and low-waste battery technology, which contributes to the energy source transition from C-, H-, and O-based material era to H- and O-based material era.

## Conflicts of interest

The authors declare no competing interests.

## Data availability

The data that support the findings of this study are available within the article. Additional supporting data are available from the corresponding authors upon reasonable request.

## Acknowledgements

The authors acknowledge Atomcent Holding AS and the Research Council of Norway (360080) for the financial support to this work.

## References

- 1 T. S. Ricketts and D. C. Elgin, Natural Gas in Scotland, *Nature*, 1957, **180**, 1444–1445, DOI: [10.1038/1801444a0](https://doi.org/10.1038/1801444a0).
- 2 R. Bailey, Problems for the Coal Industry, *Nature*, 1971, **230**, 358, DOI: [10.1038/230358a0](https://doi.org/10.1038/230358a0).
- 3 A. E. Trueman, The Coal Measures of Belgium, *Nature*, 1951, **167**, 552–553, DOI: [10.1038/167552a0](https://doi.org/10.1038/167552a0).
- 4 A. G. Sharkey, J. L. Shultz and R. A. Friedel, Gases from Flash and Laser Irradiation of Coal, *Nature*, 1964, **202**, 988–989, DOI: [10.1038/202988a0](https://doi.org/10.1038/202988a0).
- 5 C. Zahn, S. H. Langer, B. D. Blaustein and I. Wender, Optical Activity in Oils Derived from Coal, *Nature*, 1963, **200**, 53–54, DOI: [10.1038/200053a0](https://doi.org/10.1038/200053a0).
- 6 W. G. Meinschein, Y. M. Sternberg and R. W. Klusman, Origins of Natural Gas and Petroleum, *Nature*, 1968, **220**, 1185–1189, DOI: [10.1038/2201185a0](https://doi.org/10.1038/2201185a0).
- 7 J. Xie, *et al.*, Methane oxidation to ethanol by a molecular junction photocatalyst, *Nature*, 2025, **639**, 368–374, DOI: [10.1038/s41586-025-08630-x](https://doi.org/10.1038/s41586-025-08630-x).
- 8 R. W. Coughlin and M. Farooque, Hydrogen production from coal, water and electrons, *Nature*, 1979, **279**, 301–303, DOI: [10.1038/279301a0](https://doi.org/10.1038/279301a0).
- 9 T. E. Allibone, Fusion of Heavy Hydrogen, *Nature*, 1959, **183**, 569–573, DOI: [10.1038/183569a0](https://doi.org/10.1038/183569a0).
- 10 N. Hawkes, European Nuclear Energy, *Nature*, 1968, **217**, 16–17, DOI: [10.1038/217016a0](https://doi.org/10.1038/217016a0).
- 11 K. Wang, *et al.*, Lithium–antimony–lead liquid metal battery for grid-level energy storage, *Nature*, 2014, **514**, 348–350, DOI: [10.1038/nature13700](https://doi.org/10.1038/nature13700).
- 12 B. Huskinson, *et al.*, A metal-free organic–inorganic aqueous flow battery, *Nature*, 2014, **505**, 195–198, DOI: [10.1038/nature12909](https://doi.org/10.1038/nature12909).
- 13 T. Janoschka, *et al.*, An aqueous, polymer-based redox-flow battery using non-corrosive, safe, and low-cost materials, *Nature*, 2015, **527**, 78–81, DOI: [10.1038/nature15746](https://doi.org/10.1038/nature15746).
- 14 B. K. Peters, *et al.*, Scalable and safe synthetic organic electroreduction inspired by Li-ion battery chemistry, *Science*, 2019, **363**, 838–845, DOI: [10.1126/science.aav5606](https://doi.org/10.1126/science.aav5606).
- 15 Y. S. Meng, V. Srinivasan and K. Xu, Designing better electrolytes, *Science*, 2022, **378**, eabq3750, DOI: [10.1126/science.abq3750](https://doi.org/10.1126/science.abq3750).
- 16 A. C. Dillon, *et al.*, Storage of hydrogen in single-walled carbon nanotubes, *Nature*, 1997, **386**, 377–379, DOI: [10.1038/386377a0](https://doi.org/10.1038/386377a0).
- 17 H. Lee, *et al.*, Tuning clathrate hydrates for hydrogen storage, *Nature*, 2005, **434**, 743–746, DOI: [10.1038/nature03457](https://doi.org/10.1038/nature03457).
- 18 M. Peng, *et al.*, Thermal catalytic reforming for hydrogen production with zero CO<sub>2</sub> emission, *Science*, 2025, **387**, 769–775, DOI: [10.1126/science.adt0682](https://doi.org/10.1126/science.adt0682).



- 19 K. Mizushima, P. C. Jones, P. J. Wiseman and J. B. Goodenough,  $\text{Li}_x\text{CoO}_2$  ( $0 < x < 1$ ): A new cathode material for batteries of high energy density, *Mater. Res. Bull.*, 1980, **15**, 783–789, DOI: [10.1016/0025-5408\(80\)90012-4](https://doi.org/10.1016/0025-5408(80)90012-4).
- 20 Y. Chen, *et al.*, Li metal deposition and stripping in a solid-state battery via Coble creep, *Nature*, 2020, **578**, 251–255, DOI: [10.1038/s41586-020-1972-y](https://doi.org/10.1038/s41586-020-1972-y).
- 21 M.-C. Lin, *et al.*, An ultrafast rechargeable aluminium-ion battery, *Nature*, 2015, **520**, 324–328, DOI: [10.1038/nature14340](https://doi.org/10.1038/nature14340).
- 22 A. Kondori, *et al.*, A room temperature rechargeable  $\text{Li}_2\text{O}^-$ -based lithium-air battery enabled by a solid electrolyte, *Science*, 2023, **379**, 499–505, DOI: [10.1126/science.abq1347](https://doi.org/10.1126/science.abq1347).
- 23 Q. Wen, Y. Wu, X. Wang, Z. Zhuang and Y. Yu, Researches on preparation and properties of sodium polysulphide as gold leaching agent, *Hydrometallurgy*, 2017, **171**, 77–85, DOI: [10.1016/j.hydromet.2017.04.008](https://doi.org/10.1016/j.hydromet.2017.04.008).
- 24 L. Zhao, *et al.*, A Critical Review on Room-Temperature Sodium-Sulfur Batteries: From Research Advances to Practical Perspectives, *Adv. Mater.*, 2024, **36**, 2402337, DOI: [10.1002/adma.202402337](https://doi.org/10.1002/adma.202402337).
- 25 M. Wild, *et al.*, Lithium sulfur batteries, a mechanistic review, *Energy Environ. Sci.*, 2015, **8**, 3477–3494, DOI: [10.1039/C5EE01388G](https://doi.org/10.1039/C5EE01388G).
- 26 S. Klokishner, O. Reu, J. Noack, R. Schlögl and A. Trunschke, Experimental Study and Modeling of the UV-Vis and Infrared Spectra of the  $[\text{VO}(\text{O}_2)\text{H}_2\text{O}]^-$  Complex Dissolved in Water, *J. Phys. Chem. A*, 2017, **121**, 7157–7164, DOI: [10.1021/acs.jpca.7b07128](https://doi.org/10.1021/acs.jpca.7b07128).
- 27 A. Kawase, S. Shirai, Y. Yamoto, R. Arakawa and T. Takata, Electrochemical reactions of lithium-sulfur batteries: an analytical study using the organic conversion technique, *Phys. Chem. Chem. Phys.*, 2014, **16**, 9344–9350, DOI: [10.1039/C4CP00958D](https://doi.org/10.1039/C4CP00958D).

